

Aligning Diffusion Models by Optimizing Human Utility

Shufan Li^{1†}, Konstantinos Kallidromitis^{2†}, Akash Gokul^{3†*}, Yusuke Kato², and Kazuki Kozuka²

¹ University of California, Los Angeles

² Panasonic AI Research

³ Salesforce AI Research

†Equal contribution * Work done outside of Salesforce.

Correspondence to jacklishufan@cs.ucla.edu

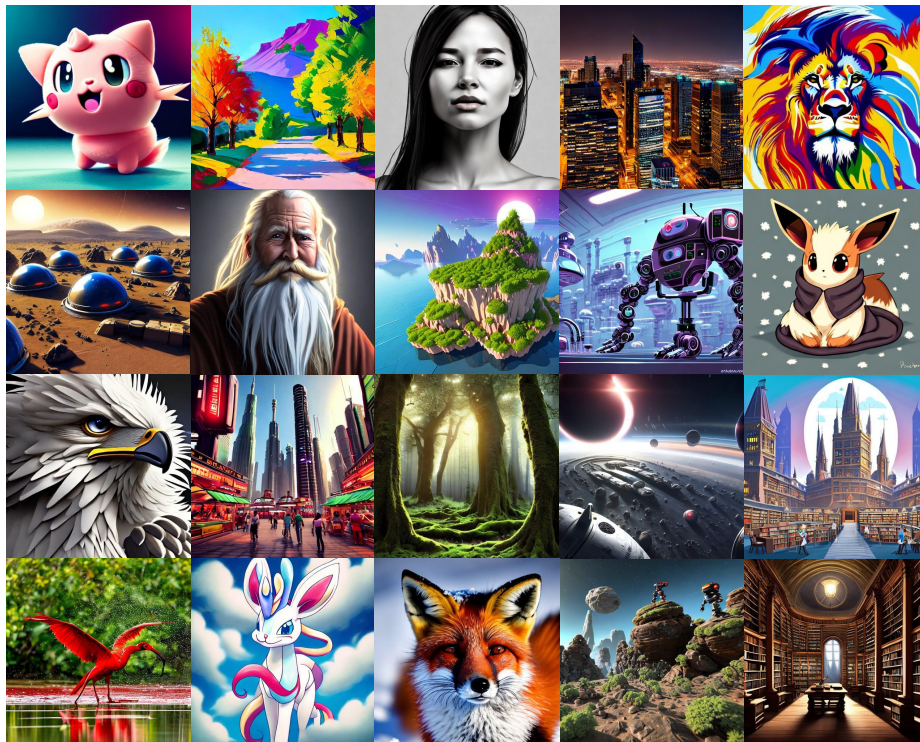


Fig. 1: Diffusion-KTO is a novel framework for aligning text-to-image diffusion models with human preference using only per-sample binary feedback. Critically, Diffusion-KTO bypasses the need to collect expensive pairwise preference data and avoids training a reward model. As seen above, Diffusion-KTO aligned text-to-image models generate images that better align with human preferences and the input prompt. We display images generated after fine-tuning Stable Diffusion v1.5 and sample prompts from HPS v2 [54], Pick-a-Pic [29], and PartiPrompts [58] datasets.

Abstract. We present Diffusion-KTO, a novel approach for aligning text-to-image diffusion models by formulating the alignment objective as the maximization of expected human utility. Since this objective applies to each generation independently, Diffusion-KTO does not require collecting costly pairwise preference data nor training a complex reward model. Instead, our objective requires simple per-image binary feedback signals, *e.g.* likes or dislikes, which are abundantly available. After fine-tuning using Diffusion-KTO, text-to-image diffusion models exhibit superior performance compared to existing techniques, including supervised fine-tuning and Diffusion-DPO [52], both in terms of human judgment and automatic evaluation metrics such as PickScore [29] and ImageReward [56]. Overall, Diffusion-KTO unlocks the potential of leveraging readily available per-image binary signals and broadens the applicability of aligning text-to-image diffusion models with human preferences.

1 Introduction

In the rapidly evolving field of generative models, aligning model outputs with human preferences remains a paramount challenge, especially for text-to-image (T2I) models. Large language models (LLMs) have made significant progress in generating text that caters to a wide range of human needs, primarily through a two-stage process of pretraining on noisy web-scale datasets followed by fine-tuning on a smaller, preference-specific dataset. The fine-tuning process aims to align the generative model’s outputs with human preferences, without significantly diminishing the capabilities gained from pretraining. Extending this fine-tuning approach to text-to-image models offers the prospect of tailoring image generation to user preferences, a goal that has remained relatively under-explored compared to its counterpart in the language domain.

Recent works have begun to explore fine-tuning text-to-image models to better align with human preferences. These methods either use a reward model, trained using human preference data, and fine-tune the T2I model to maximize reward [9, 16, 22, 30, 35, 56], or they directly fine-tune the T2I model on pairwise preference data [52, 57]. However, gathering paired preference data is an expensive and time-consuming process in which human annotators rank pairs of images according to their preferences. It is difficult to collect pairwise preference data at scale, and these datasets may be noisy as preference is subjective and, thus, varies from user to user. Additionally, training a robust reward model and fine-tuning text-to-image models using a reward model can introduce significant challenges in training, add high computational overhead in terms of memory, and limit generalization. In this work, we explore fine-tuning text-to-image diffusion models using per-image binary feedback and without requiring a reward model. While, in theory, reinforcement learning based fine-tuning methods can learn from per-image data by first training a reward model on this data, we seek to avoid training and using a reward model due to the limitations of these approaches and the success of recent works which directly fine-tune on

preference data [52]. More importantly, collecting per-image binary feedback is significantly easier than gathering pairwise preferences. This data is abundantly available as many existing social media platforms currently collect user feedback in the form of likes and dislikes. Furthermore, the simplicity and scalability of collecting such data also opens up the possibility of fine-tuning models according to the preferences of a specific user. Inspired by the large-scale applicability of learning from per-image binary feedback, we explore how to directly fine-tune text-to-image models using per-image preferences.

We address the problem of fine-tuning diffusion models from per-image binary feedback signals, *e.g.* like or dislike, by extending the human utility maximization framework used in LLMs [20] to the setting of text-to-image diffusion models. Drawing from behavioral economics, which reveals that human decision-making is not a mere mechanical process of maximizing expected rewards but is, instead, influenced by complex risk-seeking and loss-averse behaviors, KTO [20] directly optimizes LLMs according to a set of human-aware loss functions (HALOs) which encapsulate the characteristics of human decision-making. Despite only using simple per-sample binary signals to indicate desirable (+1) or undesirable (-1) outcomes, KTO fine-tuned language models perform as well as language models that are pretrained on paired preference data. This breakthrough underscores the potential of utilizing human behavioral models to align generative models. While HALOs are easy to apply to large language models, we cannot immediately apply it to diffusion models as it would require sampling across all possible trajectories in the denoising process. Although existing works approximate this likelihood by sampling once through the reverse diffusion process, this is prohibitively expensive in memory as it requires storing gradients across each step. Instead, we present a utility maximization objective, Diffusion-KTO, that extends to each step in the denoising process and thus does not require sampling through the entire reverse diffusion process. We explore various utility functions and find the Kahneman & Tversky model of human utility to perform best in aligning text-to-image diffusion models. In all, Diffusion-KTO is an easy-to-train approach to align T2I diffusion models with human preferences using only per-image binary feedback signals.

Our main contributions are as follows:

- We generalize the human utility maximization framework used to align LLMs to the setting of diffusion models (Section 4).
- Diffusion-KTO facilitates training with per-image binary feedback, avoiding the challenges in collecting pairwise preference data from users.
- Through comprehensive evaluations, we demonstrate that generations from Diffusion-KTO aligned models are generally preferred over existing approaches, as judged by human evaluators and automated metrics (Section 5.2).

In summary, Diffusion-KTO not only offers a robust framework for aligning T2I models with human preferences but also simplifies the training process and vastly expands the utility of generative models in real-world applications.

2 Related Works

2.1 Text-to-Image Generative Models

Text-to-image (T2I) models have demonstrated remarkable success in generating high quality images that maintain high fidelity to the input caption [7, 8, 13, 28, 39, 40, 58, 59]. The success of these models has not only improved image synthesis but also led to improvements in many other applications including, image editing [12] and image personalization [42]. In this work, we focus on diffusion models [26, 47, 48] due to their popularity and open-source availability. We refer the reader to Section 3.1 for more details regarding diffusion models. While text-to-image models are capable of synthesizing complex, high quality images, these models are trained on large, noisy datasets [44]. As a result, these models are not well-aligned with the preferences of human users and, thus, can often generate images with noticeable issues such as poorly rendered hands and low fidelity to the prompt. We aim to resolve these issues by introducing a fine-tuning objective that allows text-to-image diffusion models to learn directly from human preference data. We observe that fine-tuning T2I diffusion models with our objective improves image quality and image-text alignment according to human evaluators and automated metrics.

2.2 Improving Language Models using Human Feedback

Following web-scale pretraining, large language models are further improved by first fine-tuning on a curated set of data (supervised fine-tuning) and then using reinforcement learning to learn from human feedback. Reinforcement learning from human feedback (RLHF) [2, 14, 15], in particular, has been shown to be an effective means of improving the capabilities of large language models and aligning these models with user preferences [3, 5, 6, 10, 24, 31–33, 49, 63]. While this approach has been successful [1, 50], the difficulties in fine-tuning a model using RLHF [4, 19, 23, 38, 46, 53, 62] has led to the development of alternative fine-tuning objectives for alignment [20, 37, 60, 61]. Along these lines, the recently proposed KTO [20] draws inspiration from behavioral economics and introduces a fine-tuning objective that trains a LLM to maximize the utility of its output according to the Kahneman & Tversky model of human utility [51]. Critically, the utility maximization framework does not require pairwise preference data and instead only needs a binary signal, *e.g.* like or dislike, for a given sample (see Section 4). In this work, we explore aligning diffusion models given binary feedback data. As a first step in this direction, we generalize the utility maximization framework to the setting of diffusion models. We explore using various utility functions and, similar to KTO, we find the Kahneman & Tversky model to work best.

2.3 Improving Diffusion Models using Human Feedback

To date, supervised fine-tuning has been the popular strategy for improving text-to-image diffusion models. These approaches curate a dataset using some com-

combination of: preference models [34, 41], pre-trained image models [8, 18, 45, 54, 55] such as image captioning models, and human experts to filter data [17]. Here, we focus on fine-tuning text-to-image models from human preference data as it has been shown to be more effective than only supervised fine-tuning [52, 56]. However, it is important to note that supervised fine-tuning and learning from human preferences can be complementary as seen in the case of language models. In the area of aligning and improving diffusion models, many works have explored using reward models to fine-tune diffusion models via policy gradient techniques [9, 16, 21, 22, 25, 30, 35, 56]. Similar to our work, ReFL [56], DRaFT [16], and AlignProp [35] align text-to-image diffusion models to human preferences. However, these approaches require backpropagating the reward through the entire diffusion sampling process which is extremely expensive in memory. As a result, these works depend on techniques such as low-rank weight updates [27] and sampling from only a subset of steps in the reverse process, thus limiting their ability to fine-tune the model. In contrast, Diffusion-KTO uses an objective that does not require a reward model and extends to each step in the denoising process, thereby avoiding such memory issues. More broadly, the main drawbacks of these reinforcement learning based approaches are: limited generalization, *e.g.* closed vocabulary [22, 30] or reward hacking [9, 16, 35], and they depend on a potentially biased reward model. Since Diffusion-KTO trains directly on open-vocabulary preference data, we find that it is able to generalize to an open-vocabulary and avoids the biases associated with maximizing reward from a learned reward model. Recently, works such as Diffusion-DPO [52] and D3PO [57] present extensions of the DPO objective to the setting of diffusion models. Diffusion-KTO shares similarities with Diffusion-DPO and D3PO as we build upon these works to introduce a reward model-free fine-tuning objective for aligning with human preference. However, unlike these works, Diffusion-KTO uses a human utility maximization framework that does not rely on pairwise preference data and, instead, uses simple per-image binary feedback.

3 Background

3.1 Diffusion Models

Denoising Diffusion Probabilistic Models (DDPM) [26] model the image generation process as a Markovian process. Given data x_0 , the forward process gradually adds noise to x_0 by a variance schedule β_1, \dots, β_T . The state transition distribution is given by

$$q(x_t|x_{t-1}) = \mathcal{N}(x_t; \sqrt{1 - \beta_t}x_{t-1}, \beta_t\mathbf{I}) \quad (1)$$

DDPM [26] show that this process has a close form solution

$$q(x_t|x_0) = \mathcal{N}(x_t; \sqrt{\bar{\alpha}_t}x_0, (1 - \bar{\alpha}_t)\mathbf{I}) \quad (2)$$

where $\bar{\alpha}_t = \prod_{s=1}^t (1 - \beta_s)$. In the training process, we try to model the reverse process $q_\theta(x_{t-1}|x_t)$ parameterized by the neural network using the evidence lower bound (ELBO) objective:

$$\mathcal{L}_{\text{DDPM}} = \mathbb{E}_{x_0, t, \epsilon} [\lambda(t) \|\epsilon_t - \epsilon_\theta(x_t, t)\|^2] \quad (3)$$

Where $\lambda(t)$ is a time-dependent weighting function, ϵ is the added noise.

3.2 Reinforcement Learning with Human Feedback

The canonical form of Reinforcement Learning with Human feedback (RLHF) first fits a reward model on human preference data and then fine-tunes the generative model to maximize the expected reward of generation using reinforcement learning. In the reward fitting process, the typical approach of modeling human preference is the Bradley-Terry (BT) model [11], which stipulates that the posterior of human preference is given by the following formula

$$p^*(x_0 \succ x_1 | c) = \sigma(r(x_0, c) - r(x_1, c)) \quad (4)$$

where x_0, x_1 are generated samples, \succ is a preference relation, c is the condition of generation, and r is a real valued reward function. r can be parameterized by a neural network $r_\phi(x, c)$ and estimated through maximum likelihood estimation on a dataset $\mathcal{D}\{c_i, x_i^w, x_i^l\}_{i=0,1,2..}$ using the binary classification objective

$$\mathcal{L}_r(r_\phi, \mathcal{D}) = -\mathbb{E}_{c, x^w, x^l \sim \mathcal{D}} [\log \sigma(r(x_w, c) - r(x_l, c))] \quad (5)$$

Once the reward function is learned, the generative model is optimized through reinforcement learning using the reward feedback. The objective function is as follows:

$$\max_{\pi_\theta} \mathbb{E}_{c \sim \mathcal{D}, x \sim \pi_\theta(x|c)} [r(x, c)] - \beta \mathbb{D}_{\text{KL}}[\pi_\theta(x|c) || \pi_{\text{ref}}(x|c)] \quad (6)$$

where π_θ is the distribution encoded by the generative model, π_{ref} is a reference distribution. The KL-term is incorporated to prevent the model from diverging too much from the reference distribution. In practice, π_{ref} and π_θ are usually initialized with a model trained on high quality data through supervised fine-tuning.

3.3 Direct Preference Optimization

DPO [37] showed that the optimal solution of Eq. (6) π_θ^* satisfy the following equation

$$r^*(x, c) = \beta \log \frac{\pi_\theta^*(x|c)}{\pi_{\text{ref}}(x|c)} + \beta \log Z(c) \quad (7)$$

where $Z(c)$ is the partition function. Substituting $r^*(x, c)$ in Eq. (5), we can obtain an equivalent objective

$$\max_{\pi_{\theta}} \mathbb{E}_{x^w, x^l, c \sim \mathcal{D}} [\log \sigma(\beta \log \frac{\pi_{\theta}(x^w|c)}{\pi_{\text{ref}}(x^w|c)} - \beta \log \frac{\pi_{\theta}(x^l|c)}{\pi_{\text{ref}}(x^l|c)})] \quad (8)$$

Where x^w, x^l a pair of winning and losing samples and c is the condition used for generation. Through this formulation, the model π_{θ} can be directly trained in a supervised fashion without explicitly fitting a reward model.

3.4 Implicit Reward Model of Diffusion Model

One of the challenges in adapting DPO in the context of text-to-image diffusion model is that $\pi_{\theta}(x|c)$ is hard to optimize since each sample x is generated through a multi-step Markovian process. In particular, it requires computing the marginal distribution $\sum_{x_1 \dots x_N} \pi_{\theta}(x_0, x_1 \dots x_N | c)$ over all possible path of the diffusion process, where $\pi_{\theta}(x_0, x_1 \dots x_N | c) = \pi_{\theta}(x_N) \prod_{i=1}^N \pi_{\theta}(x_{i-1} | x_i, c)$.

D3PO [57] adapted DPO by considering the diffusion process as an Markov Decision Process (MDP). In this setup an agent takes an action a at each state s of the diffusion process. Instead of directly maximizing $r^*(x, c)$, one can maximize $Q^*(s, a)$ which assigns a value to each possible action at a given state in the diffusion process instead of the final outcome. In this setup, D3PO [57] showed the following relation

$$Q^*(x, c) = \beta \log \frac{\pi_{\theta}^*(a|s)}{\pi_{\text{ref}}(a|s)} \quad (9)$$

and an approximate objective for DPO:

$$\max_{\pi_{\theta}} \mathbb{E}_{s \sim d^{\pi}, a \sim \pi_{\theta}(\cdot|s)} [Q^*(s, a)] - \beta \mathbb{D}_{\text{KL}}[\pi_{\theta}(a|s) || \pi_{\text{ref}}(a|s)] \quad (10)$$

Where d^{π} is the state visiting distribution under policy π .

3.5 Expected Utility Hypothesis

In decision theory, the expected utility hypothesis assumes that a rational agent make decision based on the expected utility of all possible outcomes of an action, instead of objective measurements such as the dollar value of monetary returns. Formally, given an action a with the set of outcomes $O(a)$, the expected utility is defined as

$$EU(a) = \sum_{o \in O(a)} p_A(o) U(o) \quad (11)$$

where p_A is a subjective belief of the probability distribution of the outcomes and $U(o)$ is a real-valued function.

The prospect theory [51] further augments this model by asserting that the utility function is not defined purely on the outcome (*e.g.* the absolute gain in dollars) along, but on its relation with respect to some reference point (*e.g.* current wealth). In this formulation, the expression becomes

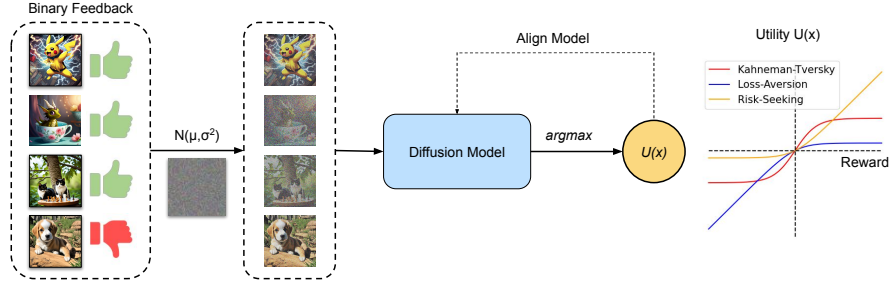


Fig. 2: We present Diffusion-KTO which aligns text-to-image diffusion models by extending the utility maximization framework to the setting of diffusion models. Since this framework aims to maximize the utility of each generation ($U(x)$) independently, it does not require paired preference data. Instead, Diffusion-KTO trains with per-image binary feedback signals, *e.g.* likes and dislikes. Our objective also extends to each step in the diffusion process, thereby avoiding the need to back-propagate a reward through the entire sampling process.

$$EU(a) = \sum_{o \in O(a)} p_A(o) U(o, o_{\text{ref}}) \quad (12)$$

Where o_{ref} is a reference outcome.

4 Method

4.1 Diffusion-KTO

Here, we propose Diffusion-KTO. Instead of optimizing the expected reward, we incorporate a non-linear utility function that calculate the utility of an action based on its value $Q^*(s, a)$ with respect to the reference point Q_{ref} .

$$\max_{\pi_{\theta}} \mathbb{E}_{s' \sim d^{\pi}, a' \sim \pi_{\theta}(\cdot|s)} [U(Q^*(s', a') - Q_{\text{ref}})] \quad (13)$$

where $U(v)$ is a monotonically increasing value function that maps the implicit reward to subjective utility. Practically, $p_{\theta}(a|s) = \pi_{\theta}(x_{t-1}|x_t)$. Applying Eq. (9), we get the objective

$$\max_{\pi_{\theta}} \mathbb{E}_{x \sim \mathcal{D}, t \sim \text{Uniform}(0, T)} [U(\beta \log \frac{\pi_{\theta}^*(x_{t-1}|x_t)}{\pi_{\text{ref}}(x_{t-1}|x_t)} - Q_{\text{ref}})] \quad (14)$$

While we do not know π^* , following KTO [20], we can optimize the policy based on whether a given generation is considered “desirable” or “undesirable”:

$$\max_{\pi_{\theta}} \mathbb{E}_{x \sim \mathcal{D}, t \sim \text{Uniform}(0, T)} [U(y(x_0)(\beta \log \frac{\pi_{\theta}^*(x_{t-1}|x_t)}{\pi_{\text{ref}}(x_{t-1}|x_t)} - Q_{\text{ref}}))] \quad (15)$$

where $y(x_0) = 1$ if x_0 is desirable and $y(x_0) = -1$ otherwise. We set $Q_{\text{ref}} = \beta \mathbb{D}_{\text{KL}}[\pi_{\theta}(a|s) || \pi_{\text{ref}}(a|s)]$. Empirically, this is calculated by computing $\max(0, \frac{1}{m} \sum \log \frac{\pi_{\theta}(a'|s')}{\pi_{\text{ref}}(a'|s')})$ over a batch of unrelated pairs of a', s' following KTO [20].

4.2 Utility Functions

While we incorporate the reference point aspect of the Kahneman-Tversky model, it is unclear if other assumptions about human behavior are applicable. It is also known that different people may exhibit different utility functions. We explore a wide range of utility functions:

Loss-Averse We characterize a loss-averse utility function as any utility function that is concave (see $U(x)$ plotted in blue in Figure 2). Particularly, if $U(x) = \log \sigma(x)$ and Q_{ref} is obtained from undesirable data, then the Diffusion-KTO objective is equivalent to the DPO objective assuming no data point appears as both desirable and undesirable. While this aligning according to this utility function follows a similar form to the DPO objective, our approach does not require paired data.

Risk-Seeking Conversely, we define a risk-seeking utility function as any convex utility function (see $U(x)$ plotted in orange in Figure 2). A typical example of a risk-seeking utility function is the exponential function. However its exploding behavior on $(+0, +\infty)$ makes it hard to optimize. Instead, for this case, we consider $U(x) = -\log \sigma(-x)$.

Kahneman-Tversky model Kahneman-Tversky’s prospect theory argues that human tend to be risk averse for gains but risk seeking for losses relative to a reference point. This amounts to a function that is concave in $(0, +\infty)$ and convex in $(0, -\infty)$. Following the adaptation proposed in KTO, we employ the sigmoid function $U(x) = \sigma(x)$ (see $U(x)$ plotted in red in Figure 2). Empirically, we find this utility function to perform best.

4.3 Subjective Probability

Under the expected utility hypothesis, the expectation is taken over the subjective belief of distribution of outcomes, not the objective distribution. In our setup, the dataset consists of unpaired samples x that are either desirable $y(x) = 1$ or undesirable $y(x) = -1$. Because we do not have access to additional information, we assume the subjective belief of a sample x is solely dependent on $y(x)$. In the training process, this translates to a biased sampling process where each sample is drawn uniformly from all desirable samples with probability γ and uniformly from all undesirable samples with probability $1 - \gamma$.

5 Experiments

We comprehensively evaluate Diffusion-KTO through quantitative and qualitative analyses to demonstrate its effectiveness in aligning text-to-image diffusion models with a preference distribution. We additionally perform synthetic experiments to highlight that Diffusion-KTO can be used to cater T2I diffusion models to the preferences of a specific user. We report the results of our ablation studies in the Appendix.

5.1 Setting

Implementation Details We fine-tune Stable Diffusion [41] v1.5 (SD v1.5) with the Diffusion-KTO objective, using the Kahneman-Tversky utility function, on the Pick-a-Pic v2 dataset [29]. The Pick-a-Pic dataset consists of paired preferences in the form (preferred image, non-preferred image) for each prompt in the dataset. Images in this dataset are generated using the Stable Diffusion series of models (fine-tuned variant of v1.5, v2.1, and SDXL [34]) and ranked by users. Since Diffusion-KTO does not require paired preference data, we partition the images in the training data. If an image has been labelled as preferred, we consider it as a desirable sample and if an image is always labelled as non-preferred, we consider it an undesirable sample. We explore other means of partitioning the training data, and provide further details, in the Appendix. In total, we train with 237,530 desirable samples and 690,538 undesirable samples. We do not train with pairwise preference data.

Evaluation We evaluate the effectiveness of aligning text-to-image diffusion models using Diffusion-KTO by comparing generations from our Diffusion-KTO aligned model to generations from existing methods using automated preference metrics and user studies. For our results using automated preference metrics, we present win-rates (how often the metric prefers Diffusion-KTO’s generations versus another method’s generations) using the LAION aesthetics classifier [43], which is trained to predict the aesthetic rating a human give to the provided image, CLIP [36], which measures image-text alignment, and PickScore [29], HPS v2 [54], and ImageReward [56] which are caption-aware models that are trained to predict human preference given an image and its caption. Additionally we perform a user study to compare Diffusion-KTO to the baseline Stable Diffusion v1.5 and the current state-of-the-art baseline, Diffusion-DPO. In our user study, we ask annotators to assess which image they prefer (*Which image do you prefer given the prompt?*) given an image generated by our Diffusion-KTO model and an image generated by the other method for the same prompt. We randomly sample prompts for each prompt style (“Animation”, “Concept-art”, “Painting”, “Photo”) from the HPS v2 [54] benchmark. We provide additional results in the Appendix.

In these evaluations, we compare Diffusion-KTO to the following baselines: Stable Diffusion v1.5 (SD v1.5), supervised fine-tuning (SFT), conditional supervised fine-tuning (CSFT), AlignProp [35], and Diffusion-DPO [52]. Our SFT

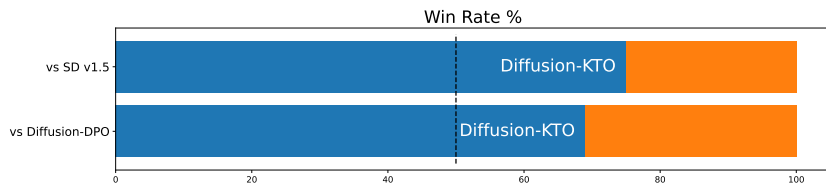


Fig. 3: User study win-rate (%) comparing Diffusion-KTO (SD v1.5) to SD v1.5 and Diffusion-DPO (SD v1.5). Results of our user study show that Diffusion-KTO significantly improves the alignment of the base SD v1.5 model. Moreover, our Diffusion-KTO aligned model also outperforms the officially released Diffusion-DPO model, as judged by users, despite only training with simple per-image binary feedback.

Method	Aesthetic	PickScore	HPS	CLIP	ImageReward
vs. SD v1.5	82.8	84.0	86.4	56.4	60.6
vs. SFT	56.0	73.0	60.6	57.6	57.2
vs. CSFT	45.8	68.6	57.4	56.8	58.2
vs. AlignProp	86.2	96.8	82.2	96.0	90.6
vs. Diffusion-DPO	70.4	59.6	74.2	48.4	49.2

Table 1: Automatic win-rate (%) for Diffusion-KTO (SD v1.5) in comparison to existing alignment approaches using prompts from the Pick-a-Pic v2 test set. In these comparisons, we use off-the-shelf models, *e.g.* preference models such as PickScore, to compare generations and determine a winner based on the method with the higher scoring generation. Diffusion-KTO (SD v1.5) drastically improves the alignment of the base SD v1.5 and demonstrates significant improvements in alignment when compared to existing approaches. Win rates above 50% are **bolded**.

baseline fine-tunes the SD v1.5 on the subset of images which are labelled as preferred using the standard denoising objective. Our CSFT baseline, similar to the approach introduced into HPS v1 [55], appends a prefix to each prompt (“good image”, “bad image”) and fine-tunes the T2I backbone using the standard diffusion objective while training with preferred and non-preferred samples independently. For AlignProp and Diffusion-DPO, we compare with their publicly released checkpoints. All baselines use Stable Diffusion v1.5.

5.2 Primary Results: Learning from Human Feedback

Quantitative Results Table 1 provides the win-rate, per automated metrics, for Diffusion-KTO aligned Stable Diffusion v1.5 and the related baselines. Diffusion-KTO substantially improves alignment for the base SD v1.5 model with win-rates of up to 86.4% according to the HPS v2 preference model (Table 1 row 1). Results from our user study (Figure 3) likewise show that human evaluators consistently prefer the generations of Diffusion-KTO to that of the base SD v1.5 (75% win-rate in favor of Diffusion-KTO). These results highlights the efficacy our alignment approach as the Diffusion-KTO aligned model bet-

ter aligns with human preference according to human evaluators and preference models such as HPS v2, PickScore (84.0% win-rate), and ImageReward (60.6% win-rate). Moreover, our method also improve image-text alignment (56.4 % win-rate using CLIP) which is a byproduct of training from preference data, as images that align with the caption are more likely to be preferred. Further, Diffusion-KTO aligned models outperform related alignment approaches such as AlignProp (Table 1 row 4) and Diffusion-DPO (Table 1 row 5). In the case of AlignProp, we find that Diffusion-KTO trained models are far more aligned with the preferred distribution as win-rates on human preference models are extremely high (96.8% PickScore, 82.2% HPS v2, 90.6% ImageReward). We attribute this to our formulation which extends the utility maximization objective to each step in the denoising and avoids the need for a reward model during training. In comparison, AlignProp requires low rank weight updates and subsampling of the diffusion chain to overcome the computational overhead introduced by their approach. Additionally, the over-saturated nature of AlignProp generations indicate that the model may be suffering from reward hacking. Lastly, we compare Diffusion-KTO to the current state-of-the-art approach for aligning diffusion model, Diffusion-DPO. Diffusion-KTO outperforms Diffusion-DPO on metrics such as Aesthetic score (70.4% win-rate), PickScore (59.6% win-rate), and HPS v2 (74.2% win-rate) while performing comparably according to other metrics. Additionally, Figure 3 shows the results of our user study that compares Diffusion-KTO with Diffusion-DPO. We find that human judges generally prefer generations from Diffusion-KTO aligned models over that of Diffusion-DPO (69% win-rate in favor of Diffusion-KTO). This highlights the effectiveness of our utility maximization objective and shows that not only can Diffusion-KTO learn from per-image binary feedback but it can also outperform models training with pairwise preference data.

Qualitative Results We showcase a visual comparison of Diffusion-KTO with existing approaches for preference alignment (Figure 4). The first prompt (row 1) requires the layout of a futuristic city, which conditions the models to show an aerial picture. Diffusion-KTO demonstrates better quality and a more sophisticated landscape compared to the other models. In the second row of images, our Diffusion-KTO aligned model is able to successfully generate a *"turtle baby sitting in a coffee cup"*. Methods such as Diffusion-DPO, in this example, have an aesthetically pleasing result but ignore key components of the prompt (*e.g.* *"turtle"*, *"night"*). On the other hand, SFT and CSFT follow the prompt but provide less appealing images. For the third prompt, which is a detailed description of a woman, the output from our Diffusion-KTO model provides the best anatomical features, symmetry, and pose compared to the other approaches. Notably, for this third prompt, the generation of the Diffusion-KTO model also generated a background is more aesthetically pleasing. The final set of images consist of a difficult prompt. It requires a lot of different objects in a niche art style. All models were able to depict the right style, *i.e.* geometric art, but the Diffusion-KTO aligned model is the only one to include the "moon," "flying fish," and

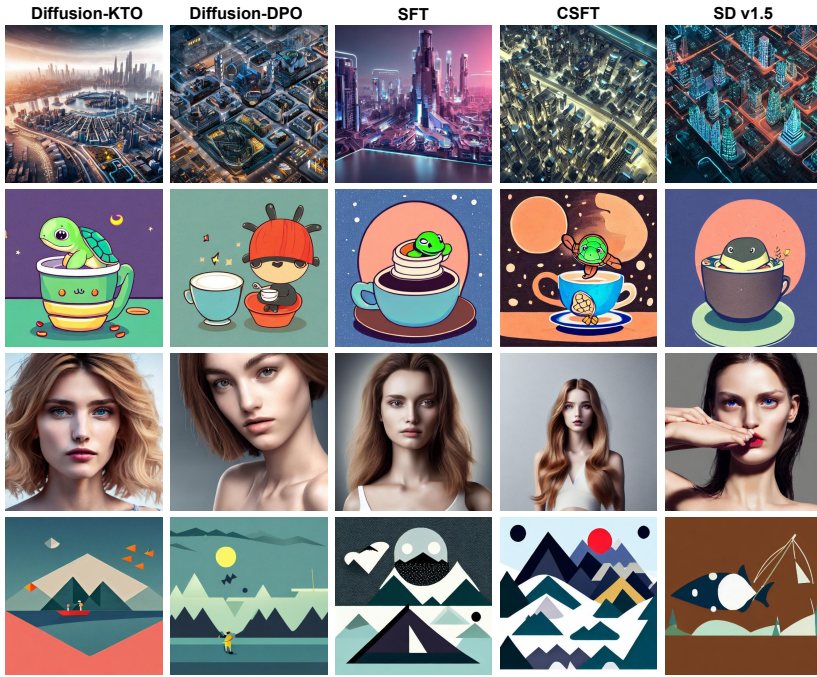


Fig. 4: Side-by-side comparison of images generated by related methods using SD v1.5. The prompts used to generate the images are: *"detailed layout of a futuristic ecologist city, high quality, cinematic lighting, sharp focus, 8k"*, *"A cute turtle baby sitting in a coffee cup, captured in an humorous illustration with warm colors and a night scenery"*, *"woman, perfect hair, perfect nose, perfect face, natural light, raytracing, perfect lips, symmetrical face, depth of field, elegant, highly detailed, octane render, denoise, photograph with a Hasselblad H3DII, extremely detailed, slim waist, long legs, fit body, healthy body, full body picture"*, *"A minimalistic fisherman in geometric design with isometric mountains and forest in the background and flying fish and a moon on top"*. Diffusion-KTO demonstrates a significant improvement in performance in terms of aesthetic appeal and fidelity to the caption.

"fisherman" objects successfully in the image. These examples demonstrate that, Diffusion-KTO is able to align the generative model not only based on visually desired characteristics such as quality and aesthetics, but also provide improve the fidelity to the prompt.

6 Synthetic Experiment: Aligning with a Specific User

Per-image binary feedback data is easy to collect and is abundantly available on the internet in the forms of likes and dislikes. This opens up the possibility of aligning T2I models to the preferences of a specific user. While users may avoid the tedious task of providing pairwise preference, Diffusion-KTO can be

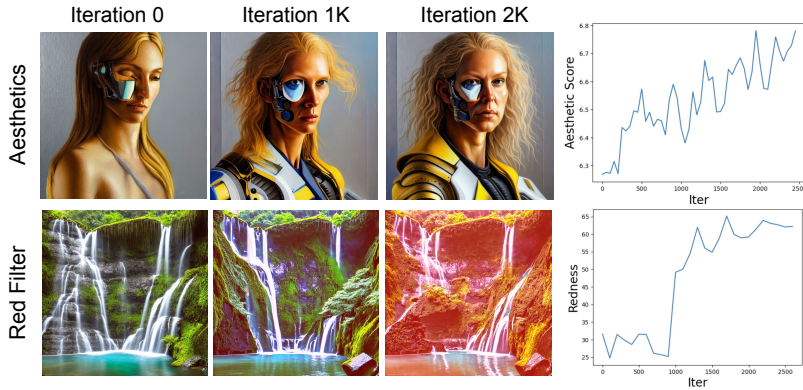


Fig. 5: Aligning text-to-image models with the preferences of a specific user. Since per-image binary feedback is easy-to-collect, we perform synthetic experiments to demonstrate that Diffusion-KTO is an effective means of aligning models to the preferences of a specific user. We show qualitative results for customizing a text-to-image model with arbitrary user preference using Diffusion-KTO Stable Diffusion v1.5. The first row displays generations from a model that is trained to learn a preference for LAION aesthetics score ≥ 7 . As expected, these generations tend to become colorful paintings. The second row displays images from a model that is trained to learn a preference for red images, and Diffusion-KTO learns to add this preference for red images while minimally changing the content of the image. We additionally plot the aesthetic score and redness score throughout the training. The redness score is calculated as the difference between the average intensity of the red channel and the average intensity in all channels.

used to easily align a diffusion model based on the images that a user likes and dislikes. Here, we conduct synthetic experiments to demonstrate that Diffusion-KTO can be used to align models to custom heuristics, in an attempt to simulate the preference of a select user.

We experiment using two custom heuristics to mock the preferences of a user. These heuristics are: (1) preference for red images (*i.e.* red filter preference) and (2) preference for images with high aesthetics score. For these experiments, we fine-tune Stable Diffusion v1.5. For the red filter preference experiment, we use (image, caption) pairs from the Pick-a-Pic v2 training set and enhance the red channel values to generate desired samples (original images are considered undesirable). For the aesthetics experiment, we train with images from the Pick-a-Pic v2 training set. We use images with an aesthetics score ≥ 7 as desirable samples and categorize the remaining images as undesirable. Figure 5 provides visual results depicting how Diffusion-KTO can align with arbitrary user preferences. For the aesthetics preference experiment (Figure 5 row 1), we see that generations exhibit higher saturation and contrast both of which are characteristics of a high scoring images per the LAION aesthetics classifier. Similarly, Diffusion-KTO also learns the preference for red images in the red filter preference experiment (Figure 5 row 2). While we experiment with simple heuristics, these results show the

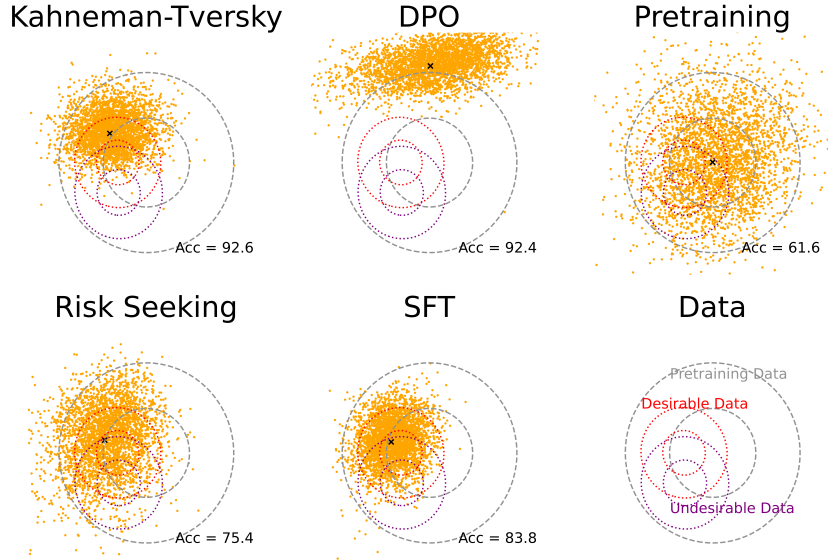


Fig. 6: Visualization of different utility functions using a toy example. We sample 3500 data points from MLP diffusion models trained using various alignment objective. Results show that Diffusion-DPO has a strong tendency to avoid loss to the point that it deviant from the distribution of positive samples. The risk seeking utility function roughly behaves the same as SFT baseline and show strong preference for positive samples at the cost of tolerating some negative samples. Diffusion-KTO achieves a good balance.

efficacy of Diffusion-KTO in learning arbitrary preferences using only per-sample binary feedback.

7 Analysis

To further study the difference between different utility functions, we conduct miniature experiments to observe their behaviors. We assume the data is two-dimensional, and the pretraining data follows a Gaussian distribution centered at $(0.5, 0.8)$ with variance 0.04. We sample desirable samples from a Gaussian distribution P_d centered at $(0.3, 0.8)$ and the undesirable drawn from a Gaussian distribution P_u centered at $(0.3, 0.6)$, and the variance of them are both 0.01. We build a small diffusion model using a MLP. We first train the model using the standard diffusion objective on the pretraining data, and then explore fine-tuning using various utility function. We sample 3500 data points from the trained model. Figure Fig. 7 shows that Diffusion-DPO has a strong tendency to avoid loss to the point that it deviates from the distribution of desirable samples. The risk seeking utility function behaves roughly the same as SFT baseline and shows a strong preference for desirable samples at the cost of tolerating some

undesirable samples. In comparison, Diffusion-KTO achieves a good balance. We also report the implicit accuracy, defined as $\mathbb{P}(P_d(x) > P_u(x))$. While both Diffusion-KTO and Diffusion-DPO achieved an accuracy above 90%, from the visualization, we observe that Diffusion-DPO clearly samples from the undesirable distribution.

8 Limitations

While Diffusion-KTO significantly improves the alignment of text-to-image diffusion models, it suffers from the shortcomings of T2I models and related alignment methods. Specifically, Diffusion-KTO is trained on preference data using prompts provided by online users and images generated using off-the-shelf T2I models. As a result, the preference distribution in this data may be skewed toward inappropriate or otherwise unwanted imagery. Additionally, since Diffusion-KTO fine-tunes a pretrained T2I model, it inherits the weaknesses of this model, including generating images that reflect negative stereotypes and images that do not align with the prompt. In spite of these limitations, Diffusion-KTO presents a broader framework for aligning diffusion models from per-image binary feedback that is applicable to any preference dataset.

9 Conclusion

In this paper, we introduced Diffusion-KTO, a novel approach to aligning text-to-image diffusion models with human preferences using a utility maximization framework. This framework avoids the need to collect costly, paired human preference data, as Diffusion-KTO only requires simple per-image binary feedback, such as likes and dislikes. We extend the utility maximization approach, which was recently introduced to align LLMs, to the setting of diffusion models and explore various utility functions. Diffusion-KTO aligned diffusion models lead to demonstrable improvements in image preference and image-text alignment when evaluated by human judges and automated metrics. While our work has empirically found the Kahneman-Tversky model of human utility to work best, we believe that the choice of utility functions remains an open question and promising direction for future work.

References

1. Achiam, J., Adler, S., Agarwal, S., Ahmad, L., Akkaya, I., Aleman, F.L., Almeida, D., Altenschmidt, J., Altman, S., Anadkat, S., et al.: Gpt-4 technical report. arXiv preprint arXiv:2303.08774 (2023) [4](#)
2. Akrou, R., Schoenauer, M., Sebag, M.: Preference-based policy learning. In: Machine Learning and Knowledge Discovery in Databases: European Conference, ECML PKDD 2011, Athens, Greece, September 5-9, 2011. Proceedings, Part I 11. pp. 12–27. Springer (2011) [4](#)
3. Askell, A., Bai, Y., Chen, A., Drain, D., Ganguli, D., Henighan, T., Jones, A., Joseph, N., Mann, B., DasSarma, N., et al.: A general language assistant as a laboratory for alignment. arXiv preprint arXiv:2112.00861 (2021) [4](#)
4. Baheti, A., Lu, X., Brahman, F., Bras, R.L., Sap, M., Riedl, M.: Improving language models with advantage-based offline policy gradients. arXiv preprint arXiv:2305.14718 (2023) [4](#)
5. Bai, Y., Jones, A., Ndousse, K., Askell, A., Chen, A., DasSarma, N., Drain, D., Fort, S., Ganguli, D., Henighan, T., et al.: Training a helpful and harmless assistant with reinforcement learning from human feedback. arXiv preprint arXiv:2204.05862 (2022) [4](#)
6. Bakker, M., Chadwick, M., Sheahan, H., Tessler, M., Campbell-Gillingham, L., Balaguer, J., McAleese, N., Glaese, A., Aslanides, J., Botvinick, M., et al.: Fine-tuning language models to find agreement among humans with diverse preferences. *Advances in Neural Information Processing Systems* **35**, 38176–38189 (2022) [4](#)
7. Balaji, Y., Nah, S., Huang, X., Vahdat, A., Song, J., Kreis, K., Aittala, M., Aila, T., Laine, S., Catanzaro, B., et al.: ediffi: Text-to-image diffusion models with an ensemble of expert denoisers. arXiv preprint arXiv:2211.01324 (2022) [4](#)
8. Betker, J., Goh, G., Jing, L., Brooks, T., Wang, J., Li, L., Ouyang, L., Zhuang, J., Lee, J., Guo, Y., et al.: Improving image generation with better captions. *Computer Science*. <https://cdn.openai.com/papers/dall-e-3.pdf> **2**(3), 8 (2023) [4](#), [5](#)
9. Black, K., Janner, M., Du, Y., Kostrikov, I., Levine, S.: Training diffusion models with reinforcement learning. arXiv preprint arXiv:2305.13301 (2023) [2](#), [5](#)
10. Böhm, F., Gao, Y., Meyer, C.M., Shapira, O., Dagan, I., Gurevych, I.: Better rewards yield better summaries: Learning to summarise without references. arXiv preprint arXiv:1909.01214 (2019) [4](#)
11. Bradley, R.A., Terry, M.E.: Rank analysis of incomplete block designs: I. the method of paired comparisons. *Biometrika* **39**(3/4), 324–345 (1952) [6](#)
12. Brooks, T., Holynski, A., Efros, A.A.: Instructpix2pix: Learning to follow image editing instructions. In: Proceedings of the IEEE/CVF Conference on Computer Vision and Pattern Recognition. pp. 18392–18402 (2023) [4](#)
13. Chang, H., Zhang, H., Barber, J., Maschinot, A., Lezama, J., Jiang, L., Yang, M.H., Murphy, K., Freeman, W.T., Rubinstein, M., et al.: Muse: Text-to-image generation via masked generative transformers. arXiv preprint arXiv:2301.00704 (2023) [4](#)
14. Cheng, W., Fürnkranz, J., Hüllermeier, E., Park, S.H.: Preference-based policy iteration: Leveraging preference learning for reinforcement learning. In: Machine Learning and Knowledge Discovery in Databases: European Conference, ECML PKDD 2011, Athens, Greece, September 5-9, 2011. Proceedings, Part I 11. pp. 312–327. Springer (2011) [4](#)
15. Christiano, P.F., Leike, J., Brown, T., Martic, M., Legg, S., Amodei, D.: Deep reinforcement learning from human preferences. *Advances in neural information processing systems* **30** (2017) [4](#)

16. Clark, K., Vicol, P., Swersky, K., Fleet, D.J.: Directly fine-tuning diffusion models on differentiable rewards. arXiv preprint arXiv:2309.17400 (2023) [2](#), [5](#)
17. Dai, X., Hou, J., Ma, C.Y., Tsai, S., Wang, J., Wang, R., Zhang, P., Vandenhende, S., Wang, X., Dubey, A., et al.: Emu: Enhancing image generation models using photogenic needles in a haystack. arXiv preprint arXiv:2309.15807 (2023) [5](#)
18. Dong, H., Xiong, W., Goyal, D., Pan, R., Diao, S., Zhang, J., Shum, K., Zhang, T.: Raft: Reward ranked finetuning for generative foundation model alignment. arXiv preprint arXiv:2304.06767 (2023) [5](#)
19. Dubois, Y., Li, C.X., Taori, R., Zhang, T., Gulrajani, I., Ba, J., Guestrin, C., Liang, P.S., Hashimoto, T.B.: AlpacaFarm: A simulation framework for methods that learn from human feedback. *Advances in Neural Information Processing Systems* **36** (2024) [4](#)
20. Ethayarajh, K., Xu, W., Muennighoff, N., Jurafsky, D., Kiela, D.: Kto: Model alignment as prospect theoretic optimization. arXiv preprint arXiv:2402.01306 (2024) [3](#), [4](#), [8](#), [9](#)
21. Fan, Y., Lee, K.: Optimizing ddpM sampling with shortcut fine-tuning. arXiv preprint arXiv:2301.13362 (2023) [5](#)
22. Fan, Y., Watkins, O., Du, Y., Liu, H., Ryu, M., Boutilier, C., Abbeel, P., Ghavamzadeh, M., Lee, K., Lee, K.: Reinforcement learning for fine-tuning text-to-image diffusion models. *Advances in Neural Information Processing Systems* **36** (2024) [2](#), [5](#)
23. Gao, L., Schulman, J., Hilton, J.: Scaling laws for reward model overoptimization. In: *International Conference on Machine Learning*. pp. 10835–10866. PMLR (2023) [4](#)
24. Glaese, A., McAleese, N., Trębacz, M., Aslanides, J., Firoiu, V., Ewalds, T., Rauh, M., Weidinger, L., Chadwick, M., Thacker, P., et al.: Improving alignment of dialogue agents via targeted human judgements. arXiv preprint arXiv:2209.14375 (2022) [4](#)
25. Hao, Y., Chi, Z., Dong, L., Wei, F.: Optimizing prompts for text-to-image generation. *Advances in Neural Information Processing Systems* **36** (2024) [5](#)
26. Ho, J., Jain, A., Abbeel, P.: Denoising diffusion probabilistic models. *Advances in neural information processing systems* **33**, 6840–6851 (2020) [4](#), [5](#)
27. Hu, E.J., Shen, Y., Wallis, P., Allen-Zhu, Z., Li, Y., Wang, S., Wang, L., Chen, W.: Lora: Low-rank adaptation of large language models. arXiv preprint arXiv:2106.09685 (2021) [5](#)
28. Kang, M., Zhu, J.Y., Zhang, R., Park, J., Shechtman, E., Paris, S., Park, T.: Scaling up gans for text-to-image synthesis. In: *Proceedings of the IEEE/CVF Conference on Computer Vision and Pattern Recognition*. pp. 10124–10134 (2023) [4](#)
29. Kirstain, Y., Polyak, A., Singer, U., Matiana, S., Penna, J., Levy, O.: Pick-a-pic: An open dataset of user preferences for text-to-image generation. *Advances in Neural Information Processing Systems* **36** (2024) [1](#), [2](#), [10](#), [21](#)
30. Lee, K., Liu, H., Ryu, M., Watkins, O., Du, Y., Boutilier, C., Abbeel, P., Ghavamzadeh, M., Gu, S.S.: Aligning text-to-image models using human feedback. arXiv preprint arXiv:2302.12192 (2023) [2](#), [5](#)
31. Menick, J., Trębacz, M., Mikulik, V., Aslanides, J., Song, F., Chadwick, M., Glaese, M., Young, S., Campbell-Gillingham, L., Irving, G., et al.: Teaching language models to support answers with verified quotes. arXiv preprint arXiv:2203.11147 (2022) [4](#)
32. Nakano, R., Hilton, J., Balaji, S., Wu, J., Ouyang, L., Kim, C., Hesse, C., Jain, S., Kosaraju, V., Saunders, W., et al.: Webgpt: Browser-assisted question-answering with human feedback. arXiv preprint arXiv:2112.09332 (2021) [4](#)

33. Ouyang, L., Wu, J., Jiang, X., Almeida, D., Wainwright, C., Mishkin, P., Zhang, C., Agarwal, S., Slama, K., Ray, A., et al.: Training language models to follow instructions with human feedback. *Advances in Neural Information Processing Systems* **35**, 27730–27744 (2022) [4](#)
34. Podell, D., English, Z., Lacey, K., Blattmann, A., Dockhorn, T., Müller, J., Penna, J., Rombach, R.: Sdxl: Improving latent diffusion models for high-resolution image synthesis. *arXiv preprint arXiv:2307.01952* (2023) [5](#), [10](#)
35. Prabhudesai, M., Goyal, A., Pathak, D., Fragkiadaki, K.: Aligning text-to-image diffusion models with reward backpropagation. *arXiv preprint arXiv:2310.03739* (2023) [2](#), [5](#), [10](#)
36. Radford, A., Kim, J.W., Hallacy, C., Ramesh, A., Goh, G., Agarwal, S., Sastry, G., Askell, A., Mishkin, P., Clark, J., et al.: Learning transferable visual models from natural language supervision. In: *International conference on machine learning*. pp. 8748–8763. PMLR (2021) [10](#)
37. Rafailov, R., Sharma, A., Mitchell, E., Manning, C.D., Ermon, S., Finn, C.: Direct preference optimization: Your language model is secretly a reward model. *Advances in Neural Information Processing Systems* **36** (2024) [4](#), [6](#)
38. Ramamurthy, R., Ammanabrolu, P., Brantley, K., Hessel, J., Sifa, R., Bauckhage, C., Hajishirzi, H., Choi, Y.: Is reinforcement learning (not) for natural language processing?: Benchmarks, baselines, and building blocks for natural language policy optimization. *arXiv preprint arXiv:2210.01241* (2022) [4](#)
39. Ramesh, A., Dhariwal, P., Nichol, A., Chu, C., Chen, M.: Hierarchical text-conditional image generation with clip latents. *arXiv preprint arXiv:2204.06125* **1**(2), 3 (2022) [4](#)
40. Ramesh, A., Pavlov, M., Goh, G., Gray, S., Voss, C., Radford, A., Chen, M., Sutskever, I.: Zero-shot text-to-image generation. In: *International Conference on Machine Learning*. pp. 8821–8831. PMLR (2021) [4](#)
41. Rombach, R., Blattmann, A., Lorenz, D., Esser, P., Ommer, B.: High-resolution image synthesis with latent diffusion models. In: *Proceedings of the IEEE/CVF conference on computer vision and pattern recognition*. pp. 10684–10695 (2022) [5](#), [10](#)
42. Ruiz, N., Li, Y., Jampani, V., Pritch, Y., Rubinstein, M., Aberman, K.: Dreambooth: Fine tuning text-to-image diffusion models for subject-driven generation. In: *Proceedings of the IEEE/CVF Conference on Computer Vision and Pattern Recognition*. pp. 22500–22510 (2023) [4](#)
43. Schuhmann, C.: Laion-aesthetics. <https://laion.ai/blog/laion-aesthetics/> (2022), accessed: 2024 - 03 - 06 [10](#)
44. Schuhmann, C., Beaumont, R., Vencu, R., Gordon, C., Wightman, R., Cherti, M., Coombes, T., Katta, A., Mullis, C., Wortsman, M., et al.: Laion-5b: An open large-scale dataset for training next generation image-text models. *Advances in Neural Information Processing Systems* **35**, 25278–25294 (2022) [4](#)
45. Segalis, E., Valevski, D., Lumen, D., Matias, Y., Leviathan, Y.: A picture is worth a thousand words: Principled recaptioning improves image generation. *arXiv preprint arXiv:2310.16656* (2023) [5](#)
46. Skalse, J., Howe, N., Krasheninnikov, D., Krueger, D.: Defining and characterizing reward gaming. *Advances in Neural Information Processing Systems* **35**, 9460–9471 (2022) [4](#)
47. Sohl-Dickstein, J., Weiss, E., Maheswaranathan, N., Ganguli, S.: Deep unsupervised learning using nonequilibrium thermodynamics. In: *International conference on machine learning*. pp. 2256–2265. PMLR (2015) [4](#)

48. Song, Y., Sohl-Dickstein, J., Kingma, D.P., Kumar, A., Ermon, S., Poole, B.: Score-based generative modeling through stochastic differential equations. arXiv preprint arXiv:2011.13456 (2020) [4](#)
49. Stiennon, N., Ouyang, L., Wu, J., Ziegler, D., Lowe, R., Voss, C., Radford, A., Amodei, D., Christiano, P.F.: Learning to summarize with human feedback. Advances in Neural Information Processing Systems **33**, 3008–3021 (2020) [4](#)
50. Touvron, H., Martin, L., Stone, K., Albert, P., Almahairi, A., Babaei, Y., Bashlykov, N., Batra, S., Bhargava, P., Bhosale, S., et al.: Llama 2: Open foundation and fine-tuned chat models. arXiv preprint arXiv:2307.09288 (2023) [4](#)
51. Tversky, A., Kahneman, D.: Advances in prospect theory: Cumulative representation of uncertainty. Journal of Risk and uncertainty **5**, 297–323 (1992) [4](#), [7](#)
52. Wallace, B., Dang, M., Rafailov, R., Zhou, L., Lou, A., Purushwalkam, S., Ermon, S., Xiong, C., Joty, S., Naik, N.: Diffusion model alignment using direct preference optimization. arXiv preprint arXiv:2311.12908 (2023) [2](#), [3](#), [5](#), [10](#), [21](#)
53. Wang, B., Zheng, R., Chen, L., Liu, Y., Dou, S., Huang, C., Shen, W., Jin, S., Zhou, E., Shi, C., et al.: Secrets of rlhf in large language models part ii: Reward modeling. arXiv preprint arXiv:2401.06080 (2024) [4](#)
54. Wu, X., Hao, Y., Sun, K., Chen, Y., Zhu, F., Zhao, R., Li, H.: Human preference score v2: A solid benchmark for evaluating human preferences of text-to-image synthesis. arXiv preprint arXiv:2306.09341 (2023) [1](#), [5](#), [10](#), [21](#)
55. Wu, X., Sun, K., Zhu, F., Zhao, R., Li, H.: Human preference score: Better aligning text-to-image models with human preference. In: Proceedings of the IEEE/CVF International Conference on Computer Vision. pp. 2096–2105 (2023) [5](#), [11](#)
56. Xu, J., Liu, X., Wu, Y., Tong, Y., Li, Q., Ding, M., Tang, J., Dong, Y.: Imagereward: Learning and evaluating human preferences for text-to-image generation. Advances in Neural Information Processing Systems **36** (2024) [2](#), [5](#), [10](#)
57. Yang, K., Tao, J., Lyu, J., Ge, C., Chen, J., Li, Q., Shen, W., Zhu, X., Li, X.: Using human feedback to fine-tune diffusion models without any reward model. arXiv preprint arXiv:2311.13231 (2023) [2](#), [5](#), [7](#)
58. Yu, J., Xu, Y., Koh, J.Y., Luong, T., Baid, G., Wang, Z., Vasudevan, V., Ku, A., Yang, Y., Ayan, B.K., et al.: Scaling autoregressive models for content-rich text-to-image generation. arXiv preprint arXiv:2206.10789 **2**(3), 5 (2022) [1](#), [4](#)
59. Yu, L., Shi, B., Pasunuru, R., Muller, B., Golovneva, O., Wang, T., Babu, A., Tang, B., Karrer, B., Sheynin, S., et al.: Scaling autoregressive multi-modal models: Pretraining and instruction tuning. arXiv preprint arXiv:2309.02591 (2023) [4](#)
60. Yuan, Z., Yuan, H., Tan, C., Wang, W., Huang, S., Huang, F.: Rrhf: Rank responses to align language models with human feedback without tears. arXiv preprint arXiv:2304.05302 (2023) [4](#)
61. Zhao, Y., Joshi, R., Liu, T., Khalman, M., Saleh, M., Liu, P.J.: Slic-hf: Sequence likelihood calibration with human feedback. arXiv preprint arXiv:2305.10425 (2023) [4](#)
62. Zheng, R., Dou, S., Gao, S., Hua, Y., Shen, W., Wang, B., Liu, Y., Jin, S., Liu, Q., Zhou, Y., et al.: Secrets of rlhf in large language models part i: Ppo. arXiv preprint arXiv:2307.04964 (2023) [4](#)
63. Ziegler, D.M., Stiennon, N., Wu, J., Brown, T.B., Radford, A., Amodei, D., Christiano, P., Irving, G.: Fine-tuning language models from human preferences. arXiv preprint arXiv:1909.08593 (2019) [4](#)

A Experiment Settings

A.1 Implementation Details

We train Stable Diffusion v1.5 (SD v1.5) on 16 NVIDIA-A100 GPUs with a batch size of 2 per GPU using the Adam optimizer. We use a base learning rate of $1e-7$ with 1000 warm-up steps for a total of 10000 iterations. We use a beta of 5000. For sampling desirable samples, we select a positive ratio (γ) of 0.8. To make Diffusion-KTO possible on preference datasets such as Pick-a-Pic [29], we create a new sampling strategy where we categorize every image that has been labelled as preferred atleast once as desirable samples and the rest as undesirable samples.

A.2 Evaluation Details

For our user studies, we employ human judges via Amazon Mechanical Turk. Judges are given the prompt and a side-by-side image consisting of two generations from two different methods (e.g. Diffusion-KTO and Diffusion-DPO [52]) for the given prompt. We gather prompts by randomly sampling 100 prompts, 25 from each prompt style (“Animation”, “Concept-art”, “Painting”, “Photo”), from the HPS v2 [54] benchmark. In the interest of human safety, we opt to use prompts from HPS v2 instead of Pick-a-Pic [29], as we have found some prompts in the latter to be suggestive or otherwise inappropriate. We gauge human preference by asking annotators which image they prefer given the prompt, *i.e.* “Which image do you prefer given the prompt?”. To ensure a fair comparison, judges are asked to select “Left” or “Right”, corresponding to which image they prefer, and they are not given any information about which methods are being compared.

For our evaluation using automated metrics, we report win-rates (how often the metric prefers Diffusion-KTO’s generations versus another method’s generations). Given a prompt, we generate one image from the Diffusion-KTO aligned model and one image using another method. The winning method is determined by which method’s image has a higher score per the automated metric. To account for the variance in sampling from diffusion models, we generate 5 images per method and report the win-rate using the median scoring images. We evaluate using all the prompts from the test set of Pick-a-Pic, the test set of HPS v2, and the prompts from PartiPrompts.

B Additional Quantitative Results

In addition to the results on the Pick-a-Pic test set reported in Table 1, we provide additional results on HPS and PartiPrompts in Tab. 2 and Tab. 3. Results show that Diffusion-KTO outperforms existing baselines on a diverse set of prompts.

Method	Aesthetic	PickScore	HPS	CLIP	ImageReward
vs. SD v1.5	70.0	74.5	72.0	53.7	54.2
vs. SFT	54.1	62.0	54.0	54.6	52.3
vs. CSFT	49.5	60.5	52.7	53.0	53.4
vs. AlignProp	83.3	96.7	78.4	91.1	86.4
vs. Diffusion-DPO	58.8	58.6	63.9	48.7	48.8

Table 2: Automatic win-rate (%) for Diffusion-KTO in comparison to existing alignment approaches using prompts from the HPS v2 test set. The provided win-rates display how often automated metrics prefer Diffusion-KTO generations to that of other methods. Win rates above 50% are **bolded**.

Method	Aesthetic	PickScore	HPS	CLIP	ImageReward
vs. SD v1.5	68.3	60.2	66.9	52.3	52.8
vs. SFT	50.3	58.6	54.7	54.2	51.4
vs. CSFT	47.3	57.0	54.2	51.6	53.1
vs. AlignProp	74.3	93.1	76.7	88.0	82.8
vs. Diffusion-DPO	59.5	48.3	59.3	48.6	48.2

Table 3: Automatic win-rate (%) for Diffusion-KTO in comparison to existing alignment approaches using prompts from PartiPrompts. The provided win-rates display how often automated metrics prefer Diffusion-KTO generations to that of other methods. Win rates above 50% are **bolded**.

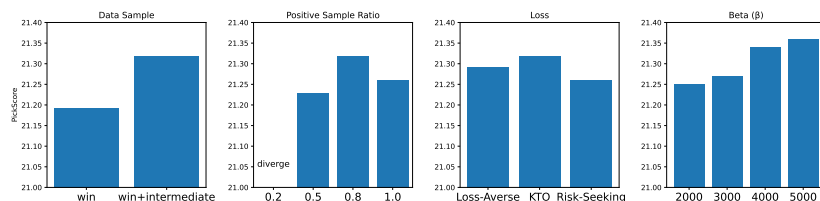


Fig. 7: Ablation Studies. We experiment with different data sampling strategy and different utility functions. Results show the best combination is to a) use the winning (*i.e.* images that are always preferred) and intermediate (*i.e.* images that are sometimes preferred and sometimes non-preferred) samples, b) use a positive ratio of 0.8, c) use the KTO objective function, d) use a beta β value of 5000.

C Ablations

We explored various design choices of Diffusion-KTO in this section. We report the mean PickScore on HPS dataset, which consists of 3500 prompts and is the largest amongst Pick-a-Pic, PartiPrompts, and HPS. We show results in Fig. 7

C.1 Data Partitioning

In converting the Pick-a-Pic dataset, which consists of pairwise preferences, to a dataset of per-image binary feedback, we consider two possible options. The first option is to categorize a sample as desired if it is always preferred across all pairwise comparisons (win), with all other samples considered undesirable. The second option additionally incorporate any samples as desirable samples if they are labelled as preferred in at least one pairwise comparison. Results show that the latter option is a better strategy.

C.2 Data Sampling

During the training process, we sample some images from the set of all desired images and some images from the set of all undesired images. This ratio is set to a fixed value γ to account for potentially imbalanced dataset. We find that sampling 80% of the images in a minibatch from the set of desired images achieves the optimal result.

C.3 Choice of β

We experiment with different values between 2000 and 5000 for β , the parameter controlling the deviation from the policy. We show that there is a rise in performance with the increase in value but with diminishing returns indicating an optimal score around 5000.

C.4 Utility function

We explored the effect of various utility function described in the main paper. Particularly, we consider Loss-Averse $U(x) = \log \sigma(x)$, KTO $U(x) = \sigma(x)$ and Risk-Seeking $U(x) = -\log \sigma(-x)$. Results show that KTO is the optimal result.

We visualize the utility function and its first order derivative in Fig. 8. Intuitively, Loss-Aversion will reduce the update step during the training when reward is sufficiently high, Risk-Seeking will reduce the update step during the training when reward is low. KTO will reduce the update step if the reward is either sufficiently high or sufficiently low. This makes KTO more robust to noisy and sometimes contradictory preferences.

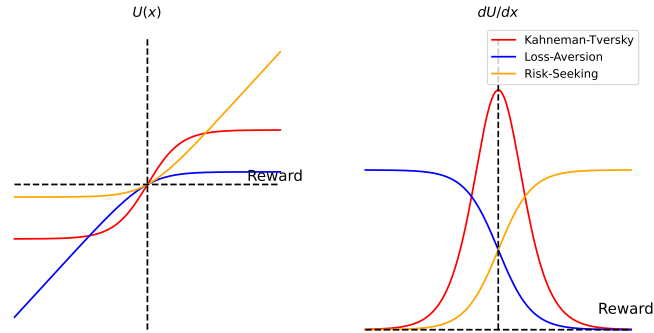


Fig. 8: Utility functions visualizations. We visualize the utility function and its first order derivative. Intuitively, Loss-Aversion will reduce the update step during the training when reward is sufficiently high, Risk-Seeking will reduce the update step during the training when reward is low. KTO will reduce the update step reward is either sufficiently high or sufficiently low. The functions are centered by a constant offset so that $U(0) = 0$ for better visibility. The constant offset does not contribute to the gradient and, thus, has no effect to training.

D Additional Qualitative Results

We provide further visual comparisons between Diffusion-KTO aligned SD v1.5 and the off-the-shelf SD v1.5 (Fig. 9, Fig. 10). We find that Diffusion-KTO aligned models improve various aspects including photorealism, richness of colors, and attention fine details. We also provide visual examples of failure cases from Diffusion-KTO aligned SD v1.5 (Fig. 11).

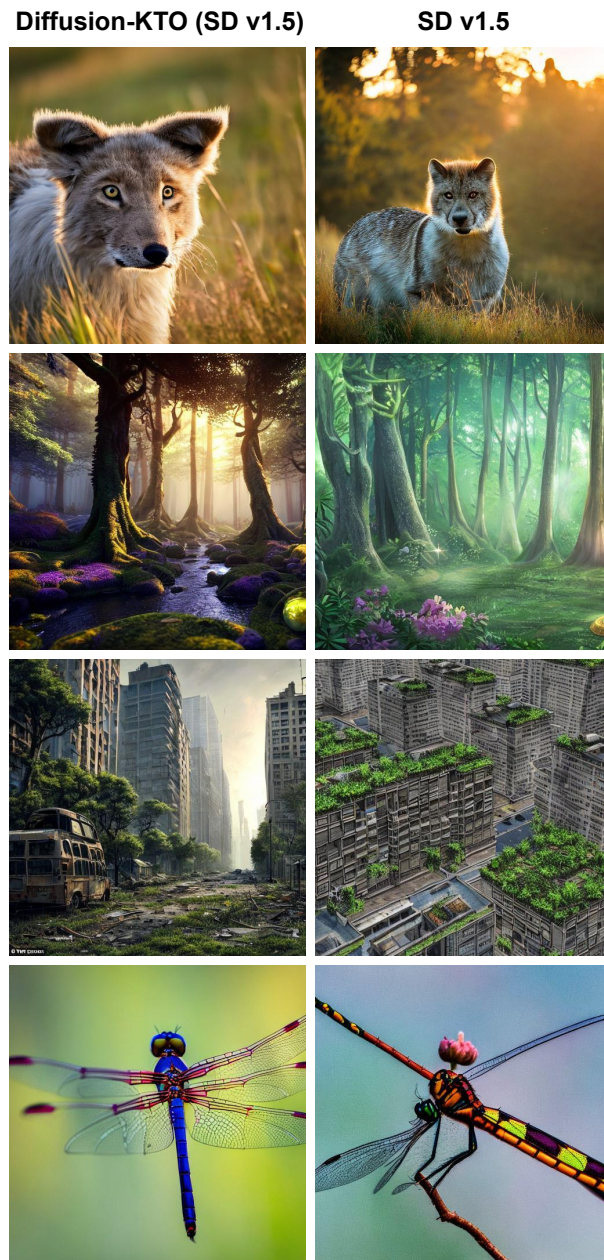


Fig. 9: Side-by-side comparison of Diffusion-KTO (SD v1.5) versus Stable Diffusion v1.5. The images were created using the prompts: "A rare animal in its habitat, focusing on its fur texture and eye depth during golden hour.", "A magical forest with tall trees, sunlight, and mystical creatures, visualized in detail.", "A city after an apocalypse, showing nature taking over buildings and streets with a focus on rebirth.", "Close-up of a dewy dragonfly, emphasizing its wings and colors."

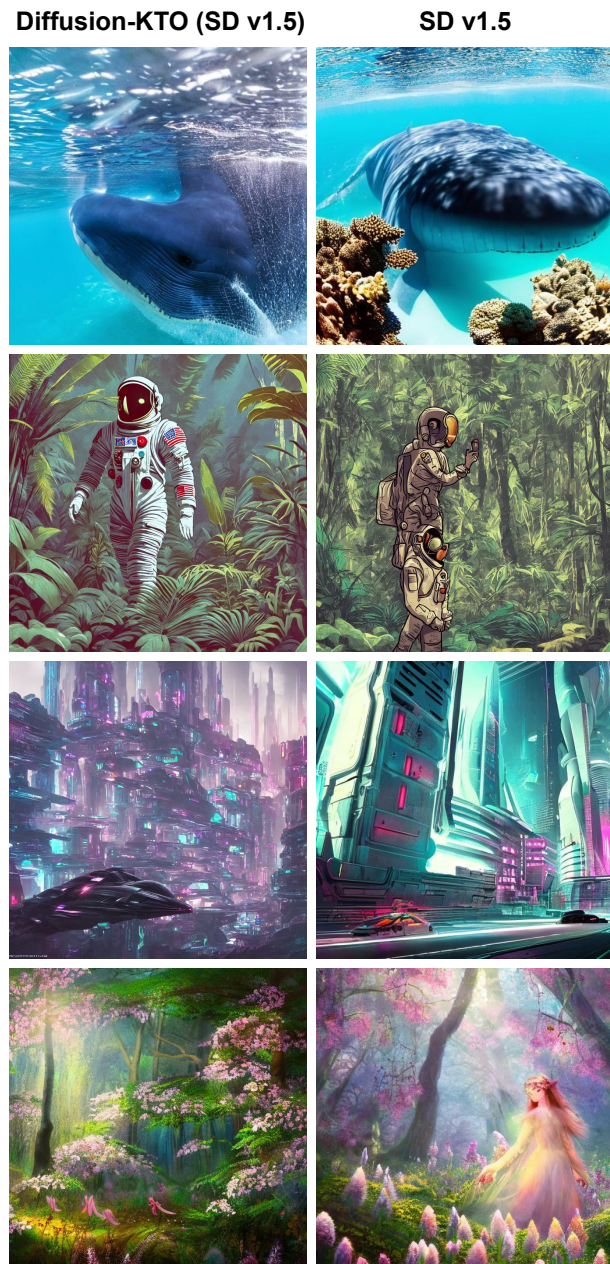


Fig. 10: Additional side-by-side comparison of Diffusion-KTO (SD v1.5) versus Stable Diffusion v1.5. The images were created using the prompts: "A close encounter with a blue whale, alongside a coral reef bustling with marine life, captured underwater in crystal-clear 8K resolution.", "Astronaut in a jungle, cold color palette, muted colors, detailed, 8k", "Futuristic spaceship and flying cars in a neon-lit city using Unreal Engine, with a cyberpunk aesthetic.", "The first bloom of spring in a magical forest where flowers emit soft light in a high-resolution fantasy painting."



Fig. 11: Failure cases of Diffusion-KTO generated using Stable Diffusion v1.5. The prompts were: "A playful dolphin leaping out of turquoise sea waves, with a backdrop of a stunningly colorful coral reef.", "An ancient dragon perched atop a mountain, overlooking a valley illuminated by the golden light of sunrise, with every scale visible in crisp detail.", "Wish you were here". In the first instance (leftmost) the dolphin is correctly shown "leaping out of the water" however, the coral reef is at the surface of the water not at the bottom of the sea. The second image shows a dragon at the top of the mountain, however the dragons body seems to merge with the stone. For the rightmost image, the caption is "Wish you were here" which is incorrectly written. It is important to note that Diffusion-KTO aligned models inherit the limitations of existing text-to-image models.